Defense Threat Reduction Agency
8725 John J. Kingman Road, MS
6201 Fort Belvoir, VA 22060-6201

DTRA-TR-13-045 (R1)

TECHNICAL REPORT

Monte-Carlo Modeling of the Prompt Radiation Emitted by a Nuclear Device in the National Capital Region, Revision 1

August 2016

Prepared by:

Human Survivability Research and
Development Integrated Program Team

REPORT DOCUMENTATION PAGE

Form Approved
OMB No. 0704-0188

1. REPORT DATE *(DD-MM-YYYY)*	**2. REPORT TYPE**	**3. DATES COVERED** *(From – To)*
10-08-2016	Technical Report	

4. TITLE AND SUBTITLE
Monte-Carlo Modeling of the Prompt Radiation Emitted by a Nuclear Device in the National Capital Region, Revision 1

5a. CONTRACT NUMBER
DTRA01-03-D-0014-0038

5b. GRANT NUMBER

5c. PROGRAM ELEMENT NUMBER

6. AUTHOR(S)
Kevin Kramer, Andy Li, Joe Madrigal, Brian Sanchez, and Kyle Millage

5d. PROJECT NUMBER

5e. TASK NUMBER

5f. WORK UNIT NUMBER

7. PERFORMING ORGANIZATION NAME(S) AND ADDRESS(ES)
AND ADDRESS(ES)
Applied Research Associates, Inc.
801 N. Quincy St., Suite 700
Arlington, VA 22203

8. PERFORMING ORGANIZATION REPORT NUMBER
DTRA-TR-13-045 (R1)

9. SPONSORING / MONITORING AGENCY NAME(S) AND ADDRESS(ES)
Defense Threat Reduction Agency
8725 John J. Kingman Road, MS 6201
Fort Belvoir, VA 22060-6201

10. SPONSOR/MONITOR'S ACRONYM(S)
DTRA J9NTSN

11. SPONSOR/MONITOR'S REPORT NUMBER(S)

12. DISTRIBUTION / AVAILABILITY STATEMENT
DISTRIBUTION A: Approved for public release; distribution is unlimited.

13. SUPPLEMENTARY NOTES

14. ABSTRACT

This document presents the results from an analysis of the impact of urban geometry on the transport of prompt radiation from a simulated low-yield nuclear device in the National Capital Region. The objective of the work was to use high-fidelity models of radiation propagation to quantify the attenuation and scattering caused by an urban landscape. The results are based on simulated data from the propagation of prompt photons and neutrons emitted from a 10-kiloton fission device, detonated at ground level, through both an open-field and urban environment. Scattered radiation from the atmosphere, ground, and urban structures is also simulated in the models. Dose output was derived from calculations using the three-dimensional Monte-Carlo radiation-transport code MCNP (Monte Carlo N-Particle). The emphasis of this report is on the radiation dose that would be received by individuals, and how that dose is perturbed by an urban environment. Consequently, radiation dose to tissue is reported, and doses are not modified to account for their relative biological effectiveness. The results shown in this report indicate the urban terrain provides significant attenuation of the prompt neutron and photon emissions, transmitting between 14-42% of the open-field dose depending on the building characteristics.

15. SUBJECT TERMS
Radiation Transport Nuclear Initial Radiation Urban Terrain Dose Estimate

16. SECURITY CLASSIFICATION OF:			**17. LIMITATION OF ABSTRACT**	**18. NUMBER OF PAGES**	**19a. NAME OF RESPONSIBLE PERSON**
a. REPORT	**b. ABSTRACT**	**a. THIS PAGE**			Paul K. Blake, PhD
U	U	U	Unlimited	40	**19b. TELEPHONE NUMBER** (include area code) *703 767-3433*

Standard Form 298 (Rev. 8-98) **Prescribed by ANSI Std. Z39.18**

UNIT CONVERSION TABLE

U.S. customary units to and from international units of measurement*

U.S. Customary Units	Multiply by → / Divide by†		International Units
Length/Area/Volume			
inch (in)	2.54	$\times 10^{-2}$	meter (m)
foot (ft)	3.048	$\times 10^{-1}$	meter (m)
yard (yd)	9.144	$\times 10^{-1}$	meter (m)
mile (mi, international)	1.609 344	$\times 10^{3}$	meter (m)
mile (nmi, nautical, U.S.)	1.852	$\times 10^{3}$	meter (m)
barn (b)	1	$\times 10^{-28}$	square meter (m^2)
gallon (gal, U.S. liquid)	3.785 412	$\times 10^{-3}$	cubic meter (m^3)
cubic foot (ft^3)	2.831 685	$\times 10^{-2}$	cubic meter (m^3)
Mass/Density			
pound (lb)	4.535 924	$\times 10^{-1}$	kilogram (kg)
unified atomic mass unit (amu)	1.660 539	$\times 10^{-27}$	kilogram (kg)
pound-mass per cubic foot (lb ft^{-3})	1.601 846	$\times 10^{1}$	kilogram per cubic meter (kg m^{-3})
pound-force (lbf avoirdupois)	4.448 222		newton (N)
Energy/Work/Power			
electron volt (eV)	1.602 177	$\times 10^{-19}$	joule (J)
erg	1	$\times 10^{-7}$	joule (J)
kiloton (kt) (TNT equivalent)	4.184	$\times 10^{12}$	joule (J)
British thermal unit (Btu) (thermochemical)	1.054 350	$\times 10^{3}$	joule (J)
foot-pound-force (ft lbf)	1.355 818		joule (J)
calorie (cal) (thermochemical)	4.184		joule (J)
Pressure			
atmosphere (atm)	1.013 250	$\times 10^{5}$	pascal (Pa)
pound force per square inch (psi)	6.984 757	$\times 10^{3}$	pascal (Pa)
Temperature			
degree Fahrenheit (°F)	[T(°F) − 32]/1.8		degree Celsius (°C)
degree Fahrenheit (°F)	[T(°F) + 459.67]/1.8		kelvin (K)
Radiation			
curie (Ci) [activity of radionuclides]	3.7	$\times 10^{10}$	per second (s^{-1}) [becquerel (Bq)]
roentgen (R) [air exposure]	2.579 760	$\times 10^{-4}$	coulomb per kilogram (C kg^{-1})
rad [absorbed dose]	1	$\times 10^{-2}$	joule per kilogram (J kg^{-1}) [gray (Gy)]
rem [equivalent and effective dose]	1	$\times 10^{-2}$	joule per kilogram (J kg^{-1}) [sievert (Sv)]

*Specific details regarding the implementation of SI units may be viewed at http://www.bipm.org/en/si/.

†Multiply the U.S. customary unit by the factor to get the international unit. Divide the international unit by the factor to get the U.S. customary unit.

Table of Contents

List of Figures

List of Tables

Revision Notes

The primary purpose of this revision is to change the flux-to-dose conversion used for neutron radiation. In the original report, the neutron dose calculations were performed using conversion coefficients from International Commision on Radiological Protection, Report 21 (ICRP-21); in this revision, the calculations are based on flux-to-dose conversion consistent with the Radiation Effects Research Foundation's Hiroshima and Nagasaki dosimetry (Radiation Effects Research Foundation 2005). The ICRP-21 (International Commission on Radiological Protection) coefficients were intended for use with low-level, occupational radiation exposure (ICRP 1973). The ICRP-21 coefficients were calculated at the maxima of the depth-dose equivalent curve, whereas the RERF flux-to-dose conversion uses kerma coefficients for soft tissue. The ICRP-21 conversion factors are more appropriate for estimating stochastic radiation effects and it overestimates neutron dose in the important contexts of consequent assessment and emergency response planning. The RERF Dosimetry System 2002 flux-to-dose conversion is more appropriate for estimating deterministic radiation effects and can be used with internal organ transmission factors such as those calculated in RERF Dosimetry System 2002.

All the figures and tables in the Results section, except for Figure 5-6, were updated with the new conversion factor. The corresponding text was also updated to describe the flux-to-dose conversion properly and to update the quantitative assessment. In addition, the photon-to-neutron dose ratio was changed to a neutron-to-photon dose ratio to make the relevant information easier to read.

We replaced the term "initial radiation" with "prompt radiation" to be more consistent with Glasstone & Dolan's The Effects of Nuclear Weapons and the nuclear weapon effects community in general. The term "initial radiation" might confuse readers into including delayed radiation effects that occur in the first minute after detonation that are not part of the neutron and photon source used in this report.

During the revision, the authors edited some of the text for clarity and for minor grammatical improvement. This version supersedes the original version dated 1 July 2013.

Section 1.

Introduction

The detonation of a low-yield nuclear weapon in a US city has been described as the one of the most critical threats we face. As a result, many federal agencies, including the Department of Defense (DoD), Department of Energy (DOE) and the Department of Homeland Security (DHS) are funding efforts to better understand the overall impacts of such an event. Within DoD, the Defense Threat Reduction Agency (DTRA) safeguards America and its allies from Weapons of Mass Destruction, chemical, biological, radiological, nuclear, and high explosives by providing capabilities to reduce, eliminate, and counter the threat and mitigate its effects. One of DTRA's research and development efforts is to understand human survivability from a nuclear weapon detonation. An integrated program team (IPT) of military, civilian, and contract scientists, known as the Human Survivability Research and Development (HSRD) IPT has been chartered to lead this effort.

Despite the multitude of above-ground nuclear testing that has occurred, the effects of urban geometry on the threat environments created by a nuclear detonation, specifically air blasts, thermal fluences, and ionizing radiation, are not well understood. This report describes an HSRD model of attenuation caused by buildings and urban terrain on the transport of the prompt radiation of a simulated nuclear detonation as defined in Glasstone and Dolan's The Effects of Nuclear Weapons (Glasstone 1977). This report does not specifically address initial radiation sources that would be emitted from the fireball and the radioactive cloud, referred to as delayed radiation, or latent radiation associated with fallout.

The neutron and photon prompt radiation presented in this report is but one of several potentially lethal prompt effects from a nuclear weapon. Injuries could also result from a variety of causes, including air blasts, building collapses, debris fragmentation, and burns. These effects may cause injury at varying distances from the detonation. Prompt radiation has the capacity to injure at long ranges, and the effects of radiation can combine with other types of injuries to increase overall lethality of a nuclear weapon detonation. Estimates of 5-15% of the people who survived the blast and thermal effects of the Hiroshima and Nagasaki attacks later died from injuries ascribed to prompt and delayed radiation (Glasstone 1977). Should a nuclear detonation occur in an urban setting similar to the setting described in this report, better knowledge of these radiation dose patterns could translate into saving thousands of people with prompt, modern medical care.

This report is organized into six sections: model description, numerical method, source description, results, discussion, and conclusions that may be drawn from the data. The report also contains a set of appendices that contain tables of more detailed interest.

Section 2.

Model Description

To calculate dose distributions in a particular environment, the HSRD model translates an urban geometry to an input file (called an 'input deck') for the MCNP radiation transport code. MCNP is a general-purpose Monte Carlo N-Particle code that can be used for neutron, photon, electron, or coupled neutron/photon/electron transport (X-5 Monte Carlo Team 2008).

The urban geometry is derived from LIDAR data which contains georeferenced building footprints and orientations, building elevations, and a representation of each building's shape at approximately 1-meter resolution. LIDAR is a commercially available, remote-sensing technology that measures distance by illuminating a target with a pulsed laser and analyzing the reflected light. The term LIDAR comes from LIght Detection And Ranging, similar to the term radar.

The urban geometries are provided by the National Geospatial-Intelligence Agency (NGA) in an ArcGIS Shapefile data format (.shp). HSRD uses a Shapefile to MCNP Input Conversion Algorithm (Shape2MCNP), an ARA, Inc. copyrighted module created for use in Esri's ArcMap™[1], to convert an entire map layer or a portion of a map layer into a three-dimensional matrix of voxels in MCNP's input format.

In the calculations presented here, the building structures for the simulations are defined by a 3-D lattice with 5-m x 5-m x 5-m voxels. For our Washington, D.C. model, an additional improvement was made by populating lattice elements of each building with different features depending on the particular building type from the Federal Emergency Management Agency (FEMA) Hazus (Hazards-US) dataset (Federal Emergency Management Agency 2003). There are sixteen different Hazus building types, though not all were used in the section of Washington, D.C. modeled. The complete list of building types in the input deck is listed in Appendix C. A representation of the lattice used in the model is shown in Figure 2-1 without the ground and air, and with each color building representing a different Hazus building type.

In the MCNP model, each building is assigned a specific Hazus building type. The assignment of Hazus values is a multistep process which begins by determining the city block (or equivalent) where the building is located. An example set of buildings with their city blocks labeled with their reference number is given in Figure 2-2. The Hazus database lists the percentage of occupancy class for each city block, and the class with the highest percentage of residency is chosen as the occupancy class for that block (if there are equal percentages, the first one in the list is chosen). To determine the building type, additional information about the region and year of origin are extracted from tables in the Hazus-MH Earthquake Technical Manual (Federal Emergency Management Agency 2003) and combined with the occupancy class. The description of our models of the Hazus building types are listed in Appendix C.

Once the building type is determined, each voxel on the exterior portion of a building is assigned exterior walls that approximate the composition and geometry of the corresponding Hazus building type. Depending on the direction the wall faces, a script is used to examine the

[1] Esri is a commercial supplier of geographic information system software and geodatabase management applications.

eight voxels that are horizontally and diagonally adjacent to each building element to decide which wall type needs to be included in that lattice element. The element is chosen from a list of 42 combinations of air and building elements as shown in Figure 2-3. For example, the 3x3 square labeled '1', in the figure, is all building interior lattice elements and the 3x3 section labeled '4' represents the NW corner of a building with air lattice elements in the top three squares and the left three squares along with building elements in the right-hand, bottom 2x2 square.

Figure 2-4 shows an example building as represented in MCNP. The figure shows the external walls with windows and gypsum drywall interior for a light-frame wood building. Ceilings are not shown. The exterior walls are represented by 1.27-cm thick wood with 0.5-cm thick glass windows. The ceilings and floors are represented by a 29.4-cm slab that approximates the bulk density of air and wood. A room with no exterior walls has four doorways, 1-m wide by 4.7-m high, each leading into a different neighboring room. The rooms on the exterior of buildings have one to three inner doors, depending on number of interior faces. The interior walls in this building type are composed of gypsum and are 2.54-cm thick. Each building type has similar levels of detail and approximations. Some types also include interior support structures, such as steel framing, inside the rooms as well.

In addition to the building lattice, atmosphere layers composed of differing air density and humidity are placed to most accurately account for sky-shine (National Aeronautics and Space Administration 1976). These layers are specific to the city's location, and their composition is described in Appendix A. The ground underlying the buildings and the spaces in between is specified to a depth of 10 m and is composed of concrete.

Other terrain features such as mountains or hills are not included in this model, though they have been added to future city models. While large variations in terrain elevation may cause a significant deviation from the results presented here, the area near the modeled detonation location in Washington, D.C. is largely level, and no major deviations are expected from using a planar terrain. The Potomac River and other bodies of water are not simulated in the model due to their distance from the detonation.

Figure 2-1. Washington, D.C. represented on a 3-D lattice model. The different colors correspond to different Hazus building types.

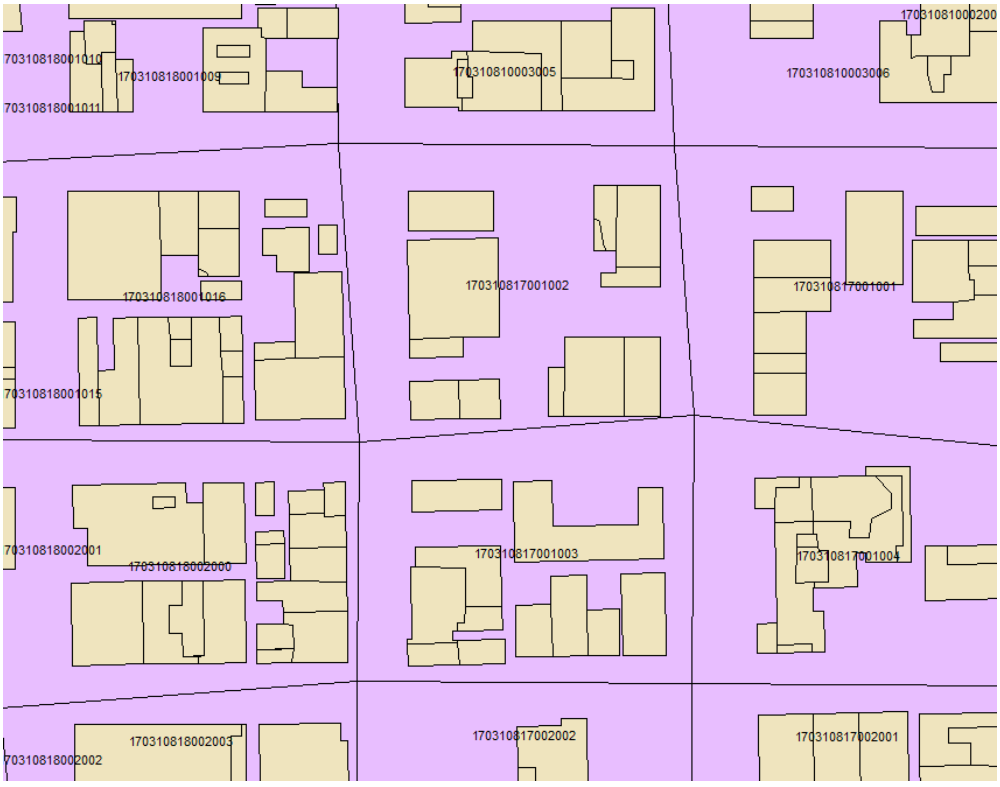

Figure 2-2. Example set of buildings and their city-block labels from the FEMA Hazus database.

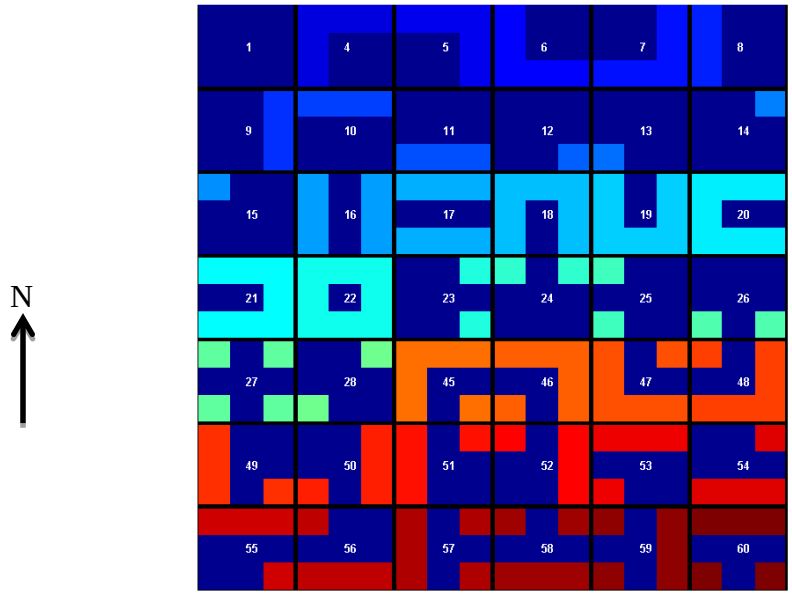

Figure 2-3. Different combinations of building and air lattice elements (numbered) which each contain different exterior wall arrangements. Building voxels are represented in dark blue, and air voxels are represented by the other colors. Exterior walls are placed where a horizontal face of a building voxel is in contact with an air voxel.

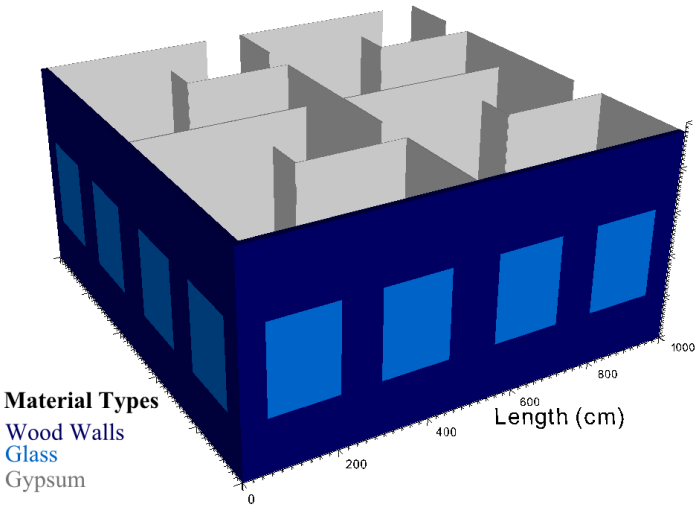

Figure 2-4. An example section of a building model representing four different 5-m x 5-m x 5-m lattice elements.

Section 3.

Numerical Methods

The simulation results presented in this report were calculated with the radiation transport code MCNP5, v1.60. The simulations were run on the Department of Defense High-Performance Computing (HPC) systems (HPC Modernization Program 2013) which are large assemblies of parallelized computer processors. For each calculation, two computational runs were performed: one with a neutron source and one with a photon source (the details of the sources are presented in the next section). Both sources were run to ten-billion event histories using the weight-windows variance-reduction technique.

On an HPC system, MCNP5 can take advantage of the message passing interface (OpenMPI) to run in parallel. Typically a single simulation of this scale, with ten-billion histories for both neutron and photon source simulations plus set-up runs, requires 6000 CPU-hours total. These statistics assure that the absorbed dose statistical error is less than 5% in areas where the total dose is greater than 0.05 Gy and less than 20% in all other areas surrounding the buildings.

MCNP5 provides a suite of variance-reduction techniques to improve the efficiency of calculations. The simulations described in this report involve transporting particles over a large 3-D space, but the tally region, where the final results are extracted, comprises only a relatively small fraction of that volume. To reduce computation time, the simulations were run with a variance-reduction technique that reduced the amount of time spent transporting particles that would not significantly contribute to the final tally count.

This technique, known as ‘weight windows’, divides the geometry into many regions and assigns each region a set of numerical bounds that describes the region’s importance to the problem. When a particle is transported into a region, its weight (loosely representing the particle flux or fluence in that area), is tested against the weight-windows bounds. If the particle’s weight is higher than the window’s upper bound, then the particle is split into several particles with lower weights that are within the bounds, conserving the total weight of the parent particle. If the particle’s weight is below the window, a random number is tested to either kill the particle or increase its weight back into the weight window (i.e. ‘Russian roulette’). If the particle is between the two weight values of the window then it is transported normally. At the end of the source particle’s history, which includes all the daughter particles transport, the contribution to the tally will automatically include the effects of this splitting and Russian roulette. With proper settings of the weights in a cylindrical weight-windows scheme, more particles are transported to regions distant to the detonation location, and thereby the statistical errors in the calculated doses are greatly decreased for a given number of source particles. This achievement is at the expense of statistical error in the region close to the detonation point, but these are typically small due to all source particles starting at a single point. Refer to the MCNP manual for a more complete description of weight-window variance-reduction methodology (X-5 Monte Carlo Team, 2008)

The bounding values of the weight windows were built using the MCNP5 weight-window generator. The simulation used to generate weight windows is created with a 1-m tall tally cell centered 1 m above the ground encircling the geometry from near the boundary. This tally records the energy deposited either by photons (if a photon source is used) or photons and neutrons (if a neutron source is used). Since both neutron and photon mesh tallies are used with

the neutron source, the weight windows for both particle types are optimized simultaneously. With weight windows, the geometry of the problem is split into concentric cylinders with the axis centered at the detonation location and oriented vertically. The spacing between cylinders is 40 m, which was chosen to be smaller than the mean free path of the typical neutron or photon in the simulation. Each volume between the cylinder surfaces is assigned a set of weight-window bounds.

To generate weight windows, the simulation is first run without any assigned weight-window bounds. This procedure results in an initial guess of the weight window bounds. The weight-window generator in MCNP5 only outputs the lower bound with the upper weight-window bound being a set as a multiple of the lower bound (the default of 2 was used). The bounds values are re-entered into the simulation and new weight windows are generated. This process is repeated until new weight-window bounds do not differ more than roughly 10% of the previous weight-window values. Then mesh tallies are placed in the simulation, and the tally used to generate the weight window is removed–at which point the input deck is ready for a production run. The mesh tallies used are discussed in Section 5.1. The weight-window bounds used with the photon source in the DC urban simulation are shown in Figure 3-1. In the figure, buildings are marked for reference, and the dark circles indicate the boundaries of each weight window cylinder.

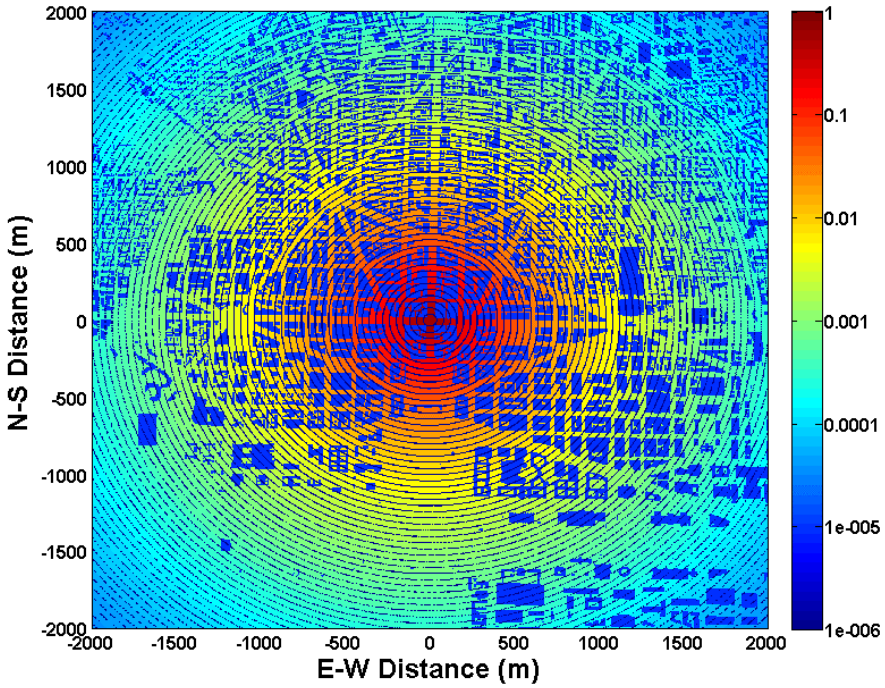

Figure 3-1. Values of weight-window lower bounds for DC urban simulation with the photon source. Buildings are represent in blue.

Section 4.

Source Description

The unclassified source spectra of initial fission neutrons and gamma rays used in the HSRD MCNP model is an isotropic version of the Hiroshima device taken from spectra provided in the Radiation Effects Research Federation (RERF) Dosimetry System 2002 (DS02) (Radiation Effects Research Foundation 2005). These neutron and gamma spectra are shown in Figure 4-1 and Figure 4-2. The Hiroshima spectra were chosen because they represents a real, but unclassified, device with more realistic prompt-radiation spectra than would idealized fission spectra. However, the spectra from the actual device are geometrically asymmetric so the energy and intensity spectra were averaged over the angular dependence to create an isotropic emission. Also, the approximate yield of the Hiroshima device was renormalized to 10 kT from its nominal yield of 16.1 kT (White 2001) to match the first scenario in the DHS national planning scenarios (DHS 2003). It should be noted that, due to the metal casing around the Hiroshima device, a considerable amount of the photon spectrum was filtered out as compared to other fission devices. The source was modeled in MCNP as a dimensionless point located 1 m above ground level at 38.902604 N latitude, 77.036574 W longitude. This is the intersection of 16th and K Street.

Table 4-1. Detail of source spectra (White 2001).

Hiroshima ("Little Boy")	Units	Value
Total neutrons	Moles/kT	0.1768
Average neutron energy	MeV	0.3106
Total gammas	Moles/kT	6.665×10^{-3}
Average gamma energy	MeV	1.3979

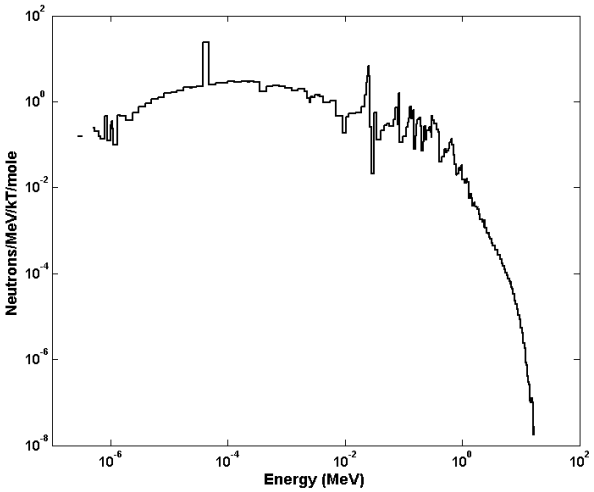

Figure 4-1. Neutron energy spectrum used in simulation. Derived from isotropic version of Little Boy bomb used at Hiroshima (White 2001).

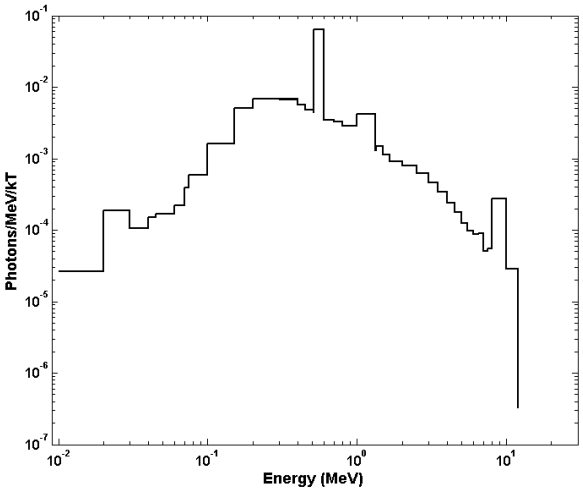

Figure 4-2. Photon energy spectrum used in simulation. Derived from isotropic version of Little Boy bomb used at Hiroshima (White 2001).

Section 5.

Results

Output dose derived from an MCNP calculation can be specified by a number of different tallies. Rectangular mesh tallies were used in the HSRD model to calculate absorbed dose (Gy) from neutrons and photons. The rectangular mesh consists of a 2202 by 2202 array of 2-m x 2-m x 1-m voxels that are centered horizontally 1.0 m above ground level (center of voxel to ground level surface). The meshes were aligned in a north to south orientation.

Results from MCNP were initially in the form of particle fluence (particles cm^{-2}), but were modified during the calculation with separate energy-dependent dose functions for neutrons and photons. Free-in-air absorbed soft-tissue dose functions from the RERF Hiroshima and Nagasaki Dosimetry in 2002 (Radiation Effects Research Foundation 2005) were used in this model. Tally values are therefore converted to absorbed dose in soft tissue: Gy.

Mesh tallies are independent of the model geometry in MCNP; i.e. a single mesh voxel may be intersected by different cells and/or materials. Therefore, doses are volume averaged within each mesh voxel. The energy-dependent dose conversion factors assume dose delivered to tissue. Values of dose evaluated in regions of building material are not doses to that specific material, but rather dose-to-tissue.

5.1 Rectangular Mesh Tally Results

The two rectangular mesh tallies provide visual representations of the propagation of neutron and photon radiation around and through the urban geometry. The sum of the two tallies is shown in Figure 5-1 for an in-the-open calculation and in Figure 5-2 for the previously described urban model. The individual neutron dose and photon dose, from both leakage photons and secondary photons from neutron interactions, are shown in Figure 5-3 and Figure 5-4. Also, doses lower than the lowest value of the scale (0.01 Gy) and higher than the highest value (10 Gy) exist but are not indicated in the figures, including values of zero where MCNP did not tally any particles in mesh voxels. It should be noted that the simulation contains only buildings, air and ground surfaces.

Figure 5-5 shows the urban-to-open ratio of the total horizontal absorbed dose. The areas where there is a building have been cut out for clarity. The plot shows that areas that have higher building elevation, the southeast section of the map for instance, are clearly attenuating the radiation more than in areas in the northeast section. Near the center and in line-of-sight from the detonation, there are increased dose levels due to albedo effects from the surrounding buildings.

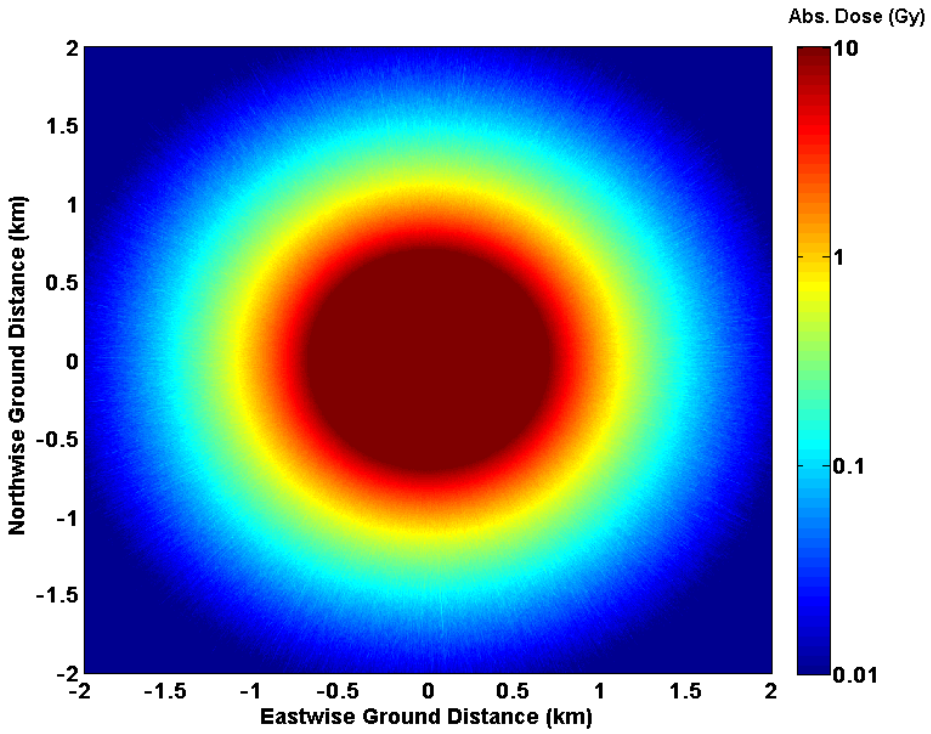

Figure 5-1. Open-field total absorbed dose.

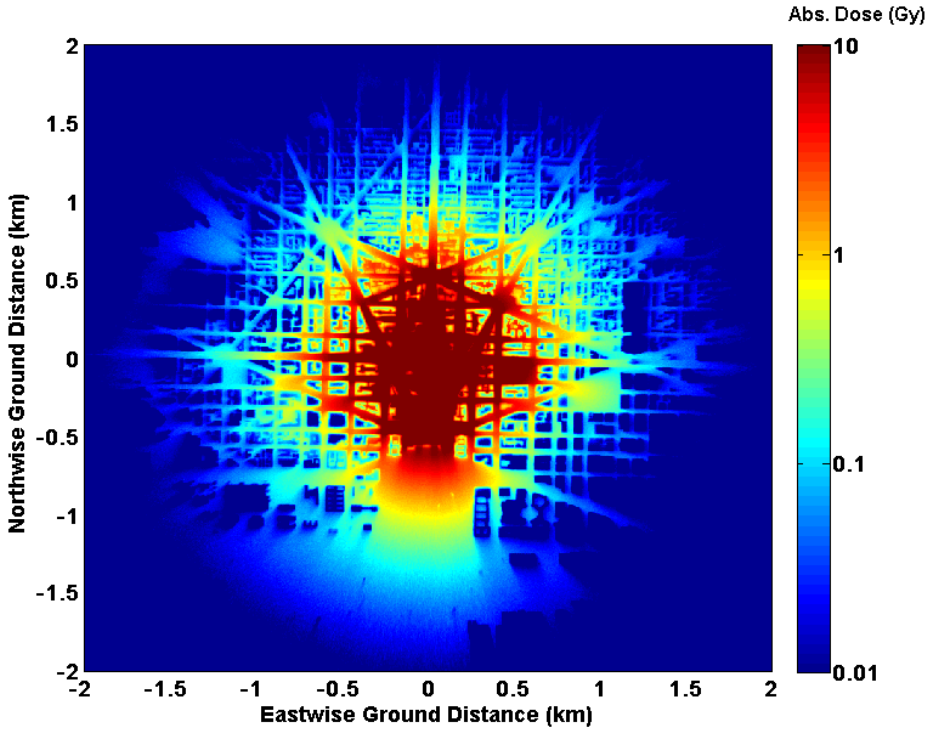

Figure 5-2. Urban total absorbed dose.

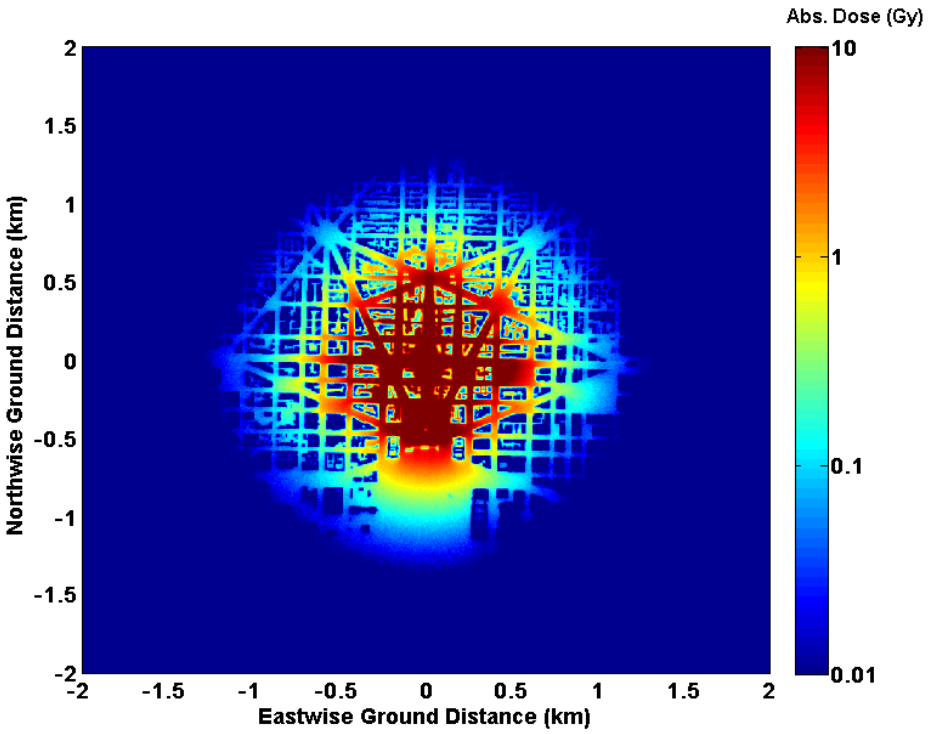

Figure 5-3. Urban neutron absorbed dose.

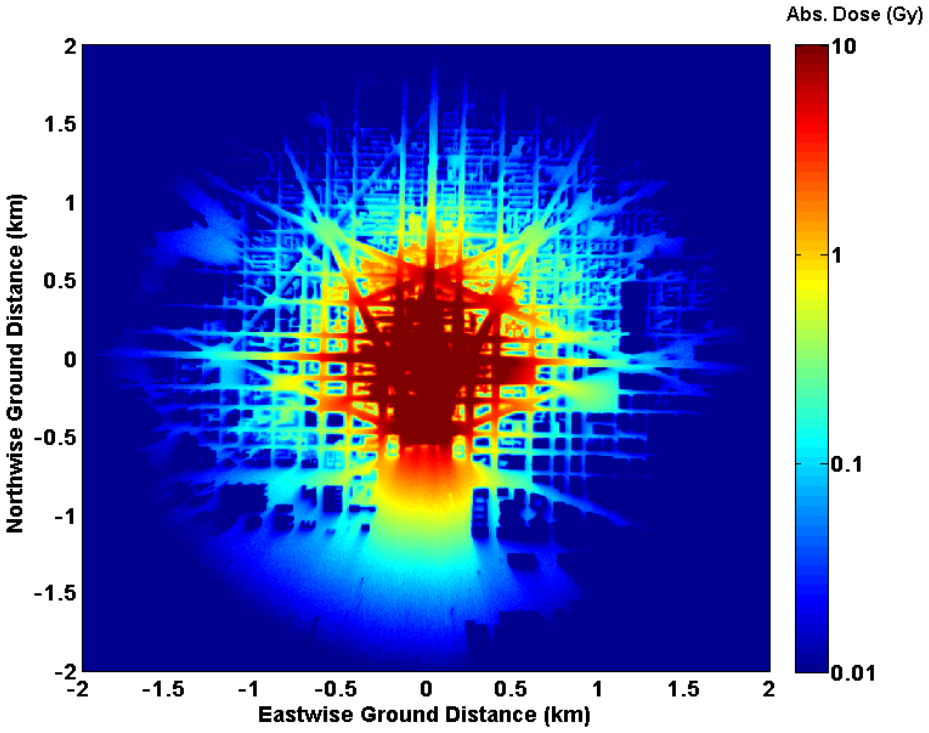

Figure 5-4. Urban photon absorbed dose from both leakage photons and secondary photons from neutron interactions.

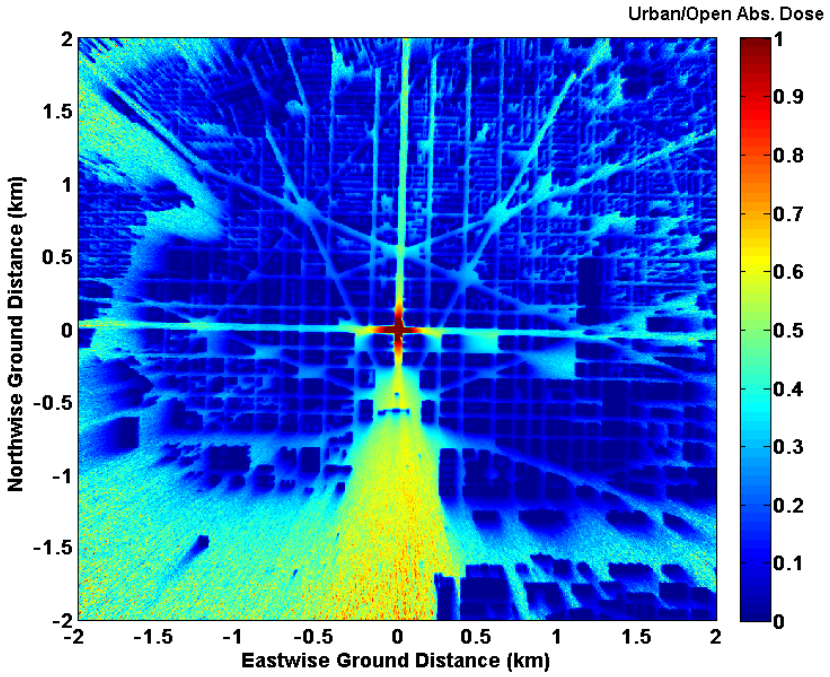

Figure 5-5. The ratio of urban horizontal absorbed dose to open-field horizontal absorbed dose.

5.2 Data Analysis

To understand the heterogeneous nature of prompt radiation in an urban environment, it is useful to look at dose distributions at constant distances from the detonation point. In this analysis, we are more interested in the dose outside of buildings rather than inside. The model provides a detailed representation of building shapes and sizes, and has a reasonable estimate of the building interiors. The variance-reduction methods used in this analysis optimized the calculations to estimate the dose to individuals outside of the buildings, so the dose estimates inside of buildings are not of sufficient fidelity. However, future work could include using these same models with different variance-reduction methods to estimate doses inside buildings.

Tally results were determined using the 2-m x 2-m rectangular mesh tally at 1 m, and a MATLAB® script was used to calculate the doses at specific geometric locations. Figure 5-6 shows a building-height map of the National Capital Region (NCR), including a set of yellow lines used to illustrate the different quadrants in the analysis that demonstrate the effect of the heterogeneous urban environment. Areas in the footprint of buildings are excluded from the sample.

Figure 5-7 shows the dose fall-off in the open-field and in the urban environment. The doses in the urban scenario exclude doses inside buildings. Figure 5-8 shows the average over all four quadrants of the total urban-to-open field dose ratio outside building structures as a function of distance. The values of Figure 5-8 are also given in Table 5-1, showing the percent to which the dose is reduced in the urban landscape as compared to the open field.

The heterogeneous nature of the data is amply demonstrated in Figure 5-9 and Figure 5-10. These plots show the Urban/Open ratio at individual points along circles at radii of 500 m and 1200 m from the detonation. The x axes correspond to the angles (degrees) at which the segments of the mesh tallies are situated. The 0^{th} degree is aligned with the north compass direction and angles advance clockwise. Figure 5-11 and Figure 5-12 show the variation of the urban-to-open field total absorbed dose ratio at 500 m and 1200 m, respectively. The initial peak in the ratio originates in the north, east and west quadrants, and the second higher peak represents the emptier parts of the south quadrant.

Figure 5-13 shows the neutron-to-photon ratio of doses in urban and open-field. The graph shows the radii at average values of the external neutron dose to the external photon dose in the range of biologically relevant values. The LD50/60 level (4.10 Gy) is considered to be where 50% of the exposed population will die within 60 days of exposure (Anno, et al. 2003). The asymptomatic level (0.75 Gy) is considered the lower dose threshold of the presence of symptoms from acute radiation syndrome (Goetz 1979). As shown in the graph, the external-to-buildings neutron-to-photon dose ratio in the urban environment is between 0.85 and 0.55 in the dose domain of 4.1 Gy to 0.75 Gy.

Figure 5-14 is a graph of the total dose fall-off as a function of the distance from the detonation point. The graph shows the dose in each of the individual four directional quadrants mentioned in Figure 5-6. Table 5-2 shows a list of interpolated distances from the detonation point at which the dose is at a point of biological interest. The pathways with more direct line of sight or with significant open space, for instance in the south quadrant, will have less dramatic dose fall-offs than those that mostly consist of urban building structures.

The differences in the biological effects of neutron radiation as compared to photon radiation are known but difficult to quantify, as the literature on neutron deterministic effects is sparse. Therefore, in this report the authors use the sum of free-in-air soft-tissue neutron and photon dose as the total dose. Correction factors for the relative biological effectiveness or interior organ transmission have not been applied. The three color regions shown in Figure 5-15 refer to high probability of lethal dose from prompt radiation (shown in red, defined as > 4.1-Gy equivalent dose), high probability of acute injury due to prompt radiation (shown in yellow, > 0.75-Gy equivalent dose) and low probability of acute injury from prompt radiation alone (shown in green, < 0.75-Gy equivalent dose).

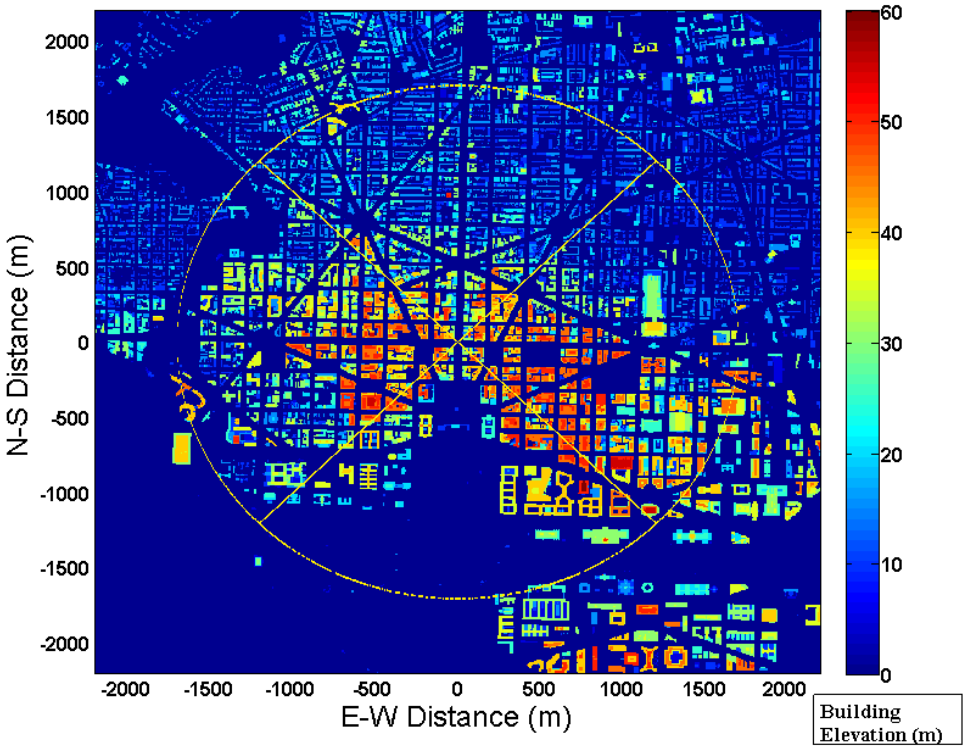

Figure 5-6. The model's city geometry showing the buildings used to calculate the outside-of-building dose.

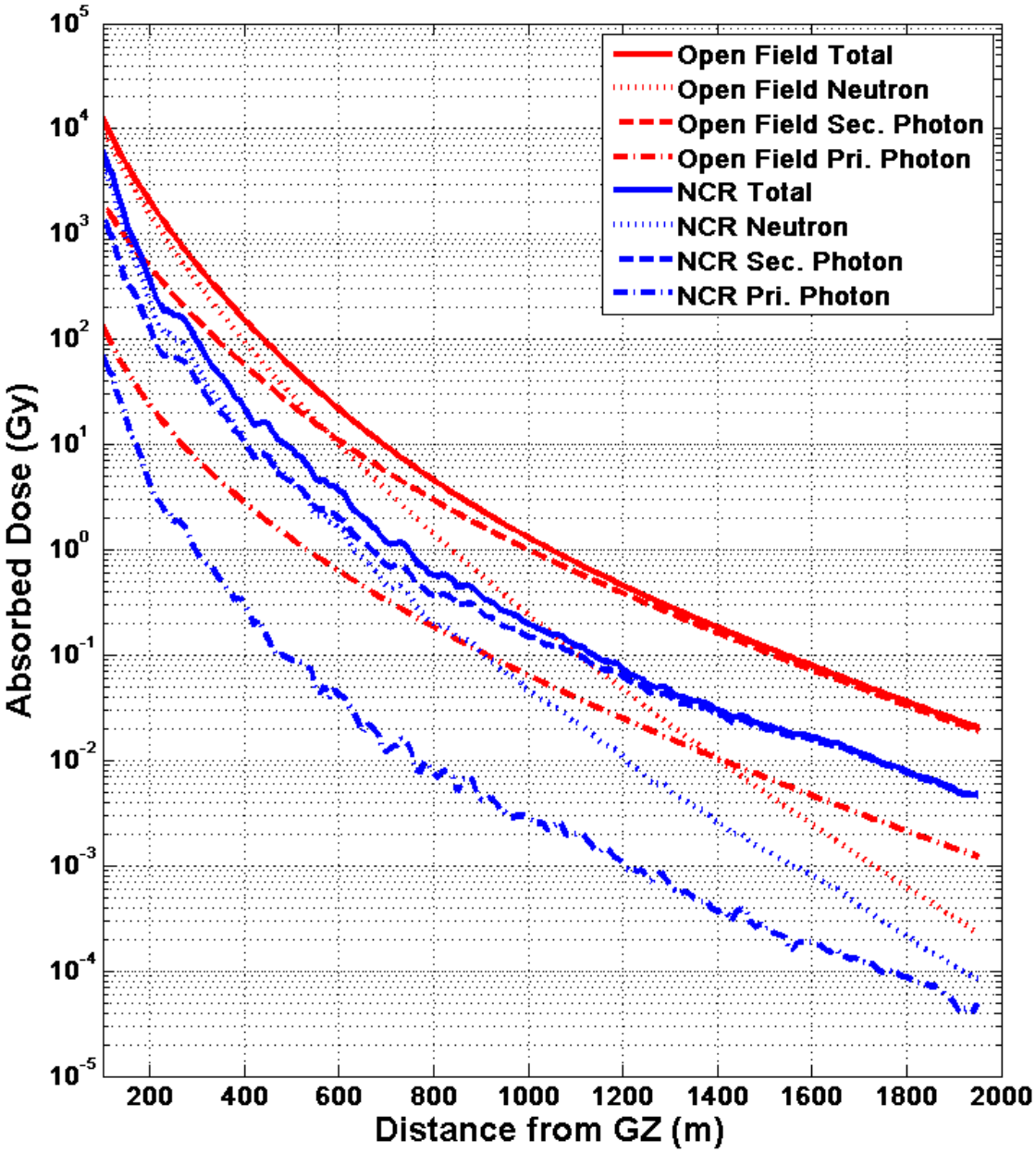

Figure 5-7. Open and outside-of-buildings urban scenario dose fall-offs.

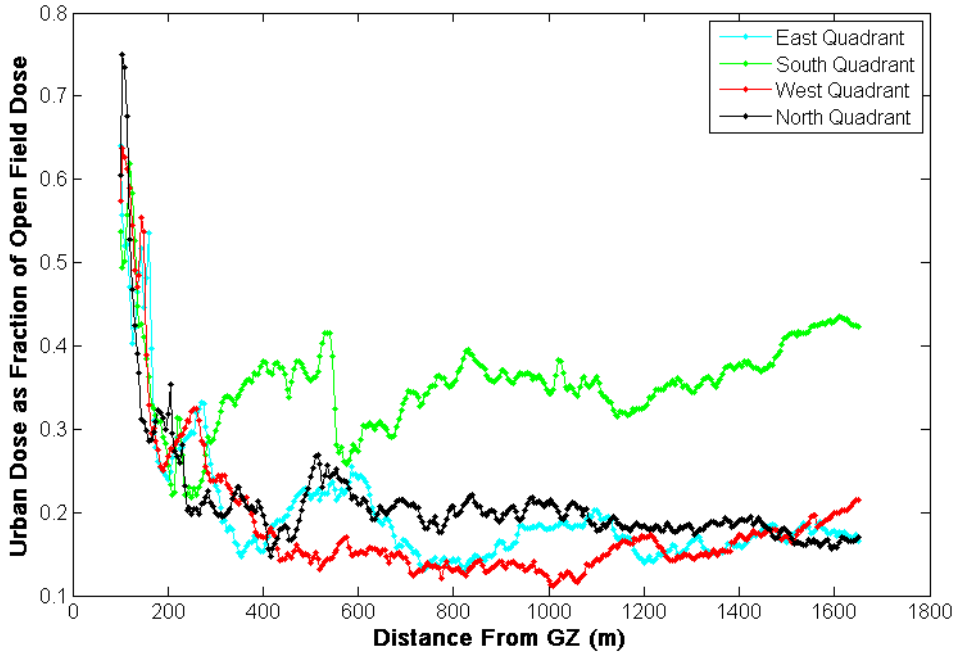

Figure 5-8. Total urban-to-open field dose ratio at locations outside buildings for the four quadrants from Figure 5-6.

Table 5-1. Values for outside-of-buildings total dose ratio, converted to percentages.

	East Quadrant	South Quadrant	West Quadrant	North Quadrant
Distance (m)	Urban-to-Open Ratio	Urban-to-Open Ratio	Urban-to-Open Ratio	Urban-to-Open Ratio
200	23.93%	25.64%	26.66%	31.83%
300	23.16%	29.83%	23.85%	19.90%
400	15.24%	38.13%	16.98%	19.68%
500	21.62%	35.86%	13.96%	24.23%
600	24.05%	27.28%	15.00%	20.95%
700	16.63%	33.67%	14.48%	21.12%
800	14.45%	35.57%	13.02%	20.70%
900	16.47%	37.00%	14.15%	19.11%
1000	18.04%	34.34%	11.77%	21.05%
1100	20.20%	36.25%	14.34%	17.76%
1200	13.93%	32.59%	17.02%	18.44%
1300	16.49%	34.37%	14.59%	18.08%
1400	16.05%	37.78%	17.36%	19.08%
1500	16.43%	41.03%	17.16%	17.81%
1600	17.75%	42.95%	19.87%	15.86%
Average	18.30%	34.82%	16.68%	20.37%

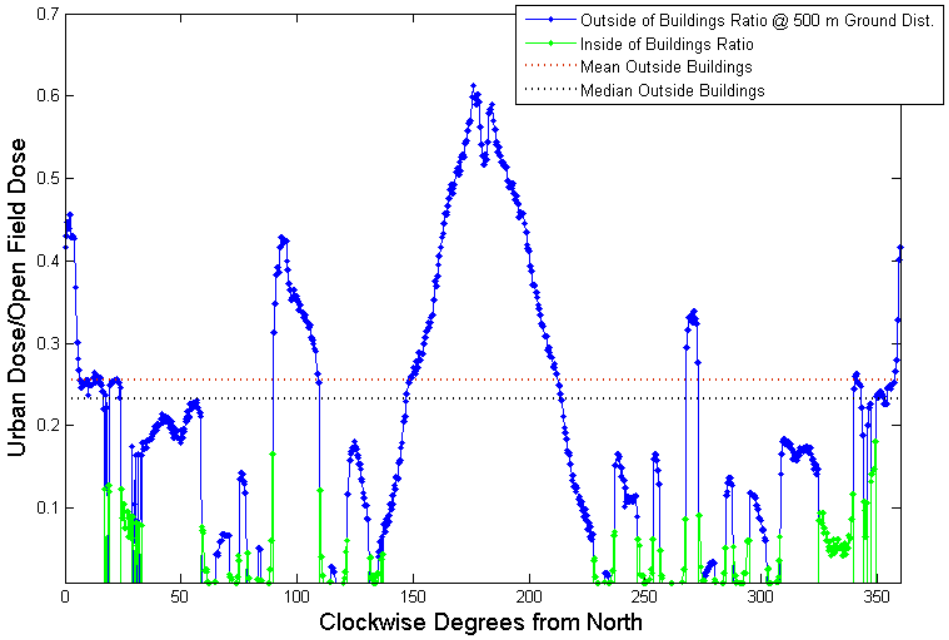

Figure 5-9. Plotted ratio of Urban-to-Open field dose at 500-m radius from the detonation point, with points over building footprints in green.

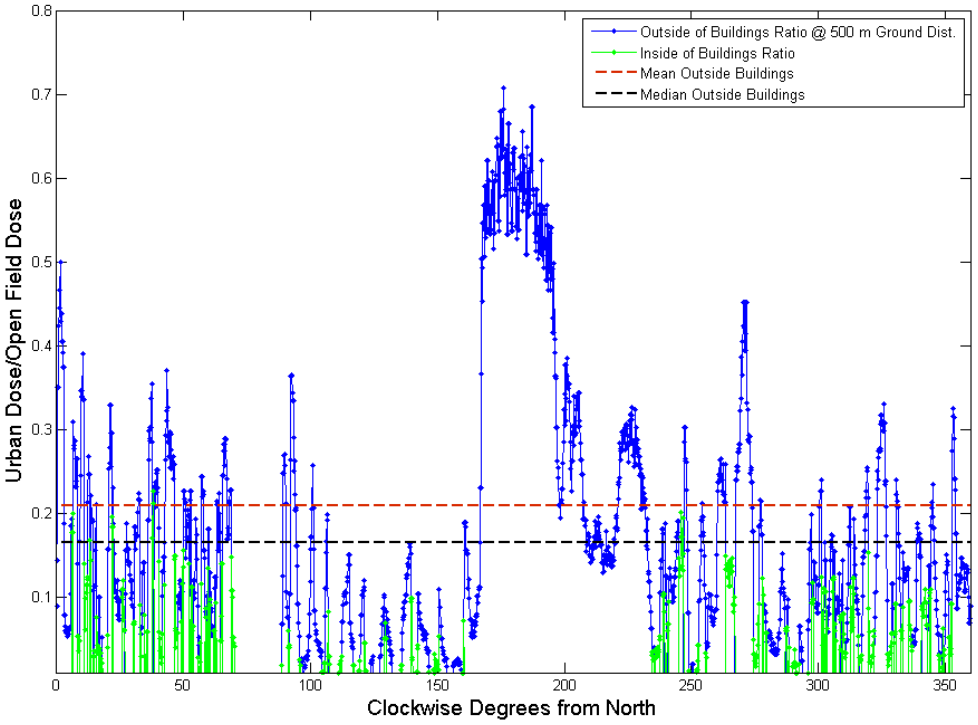

Figure 5-10. Plotted ratio of Urban-to-Open field dose at 1200-m radius from the detonation point, with points over building footprints in green.

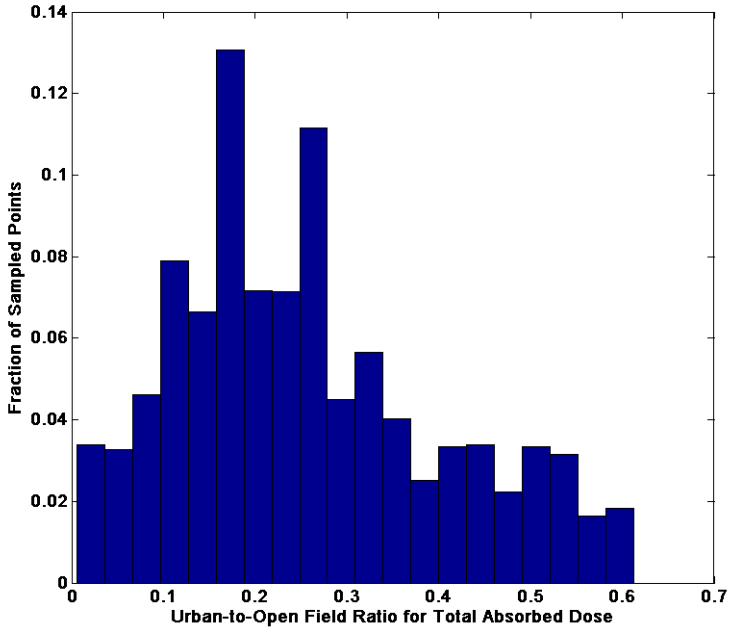

Figure 5-11. Variation of Urban-to-Open Field Total Absorbed Dose Ratio at 500 m from detonation location.

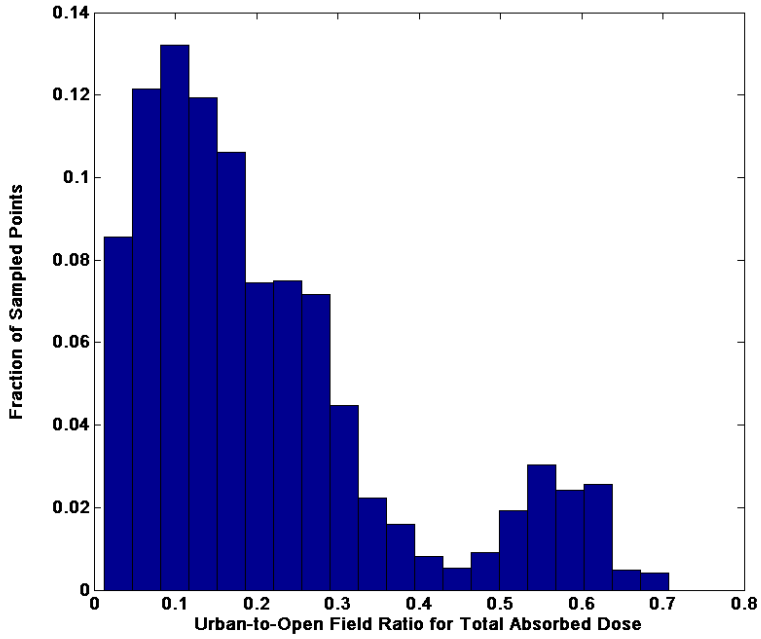

Figure 5-12. Variation of Urban-to-Open Field Total Absorbed Dose Ratio at 1200 m from detonation location.

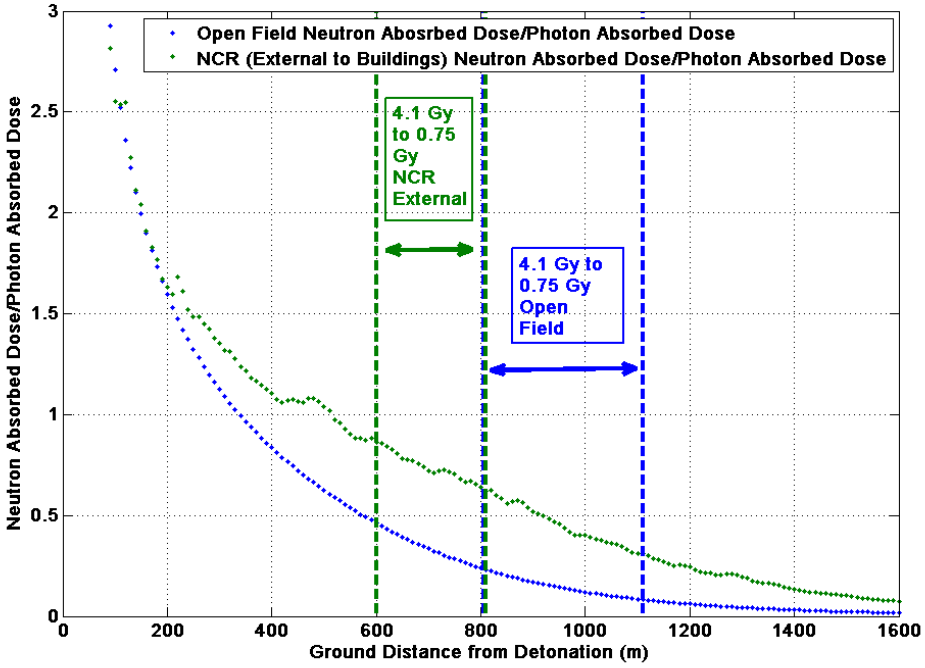

Figure 5-13. Neutron-to-Photon absorbed dose for urban (external to buildings) and open field with biologically relevant regions marked.

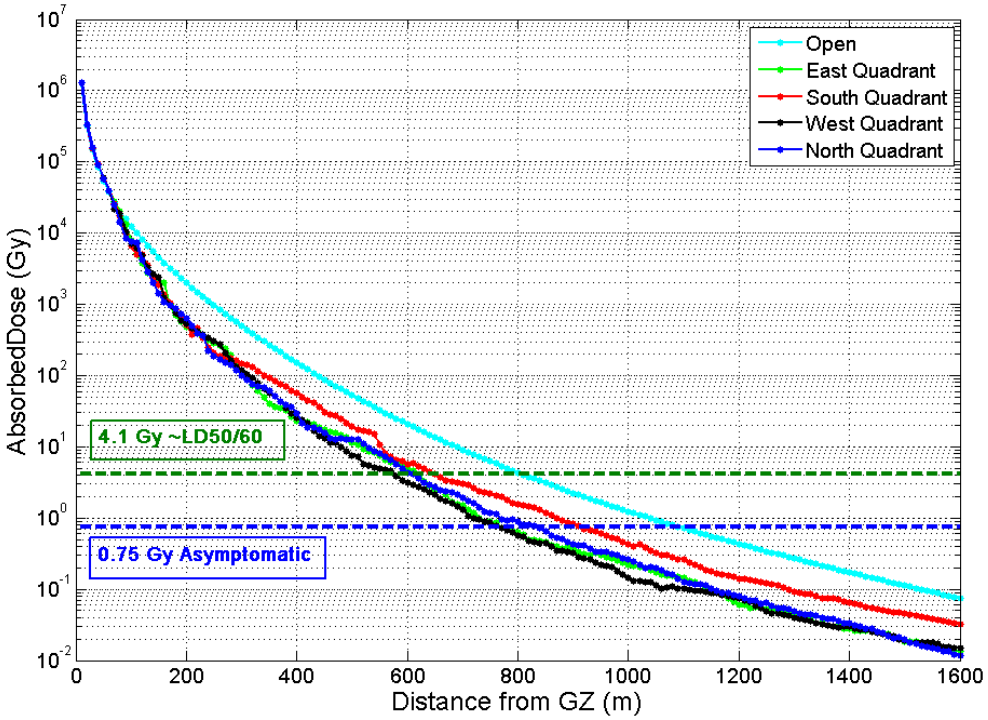

Figure 5-14. Total dose fall off for different quadrants compared to open-field calculation.

Table 5-2. Distance from detonation point to the LD50/60 and asymptomatic dose levels for the four urban quadrants and the open field calculations.

		Quadrants of NRC			
Dose (Gy)	Open Field (m)	East (m)	South (m)	West (m)	North (m)
4.10 (~LD50/60)	810	550	650	585	610
0.75 (~Asymptomatic)	1090	770	910	765	835

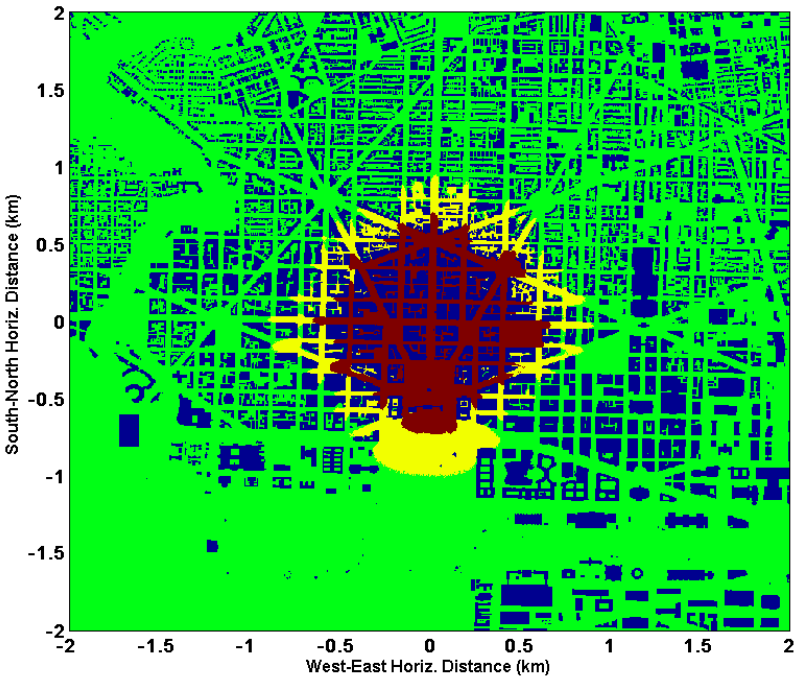

Figure 5-15. Dose map of Washington, DC showing areas of likely lethal levels of prompt radiation (red, > 4.1 Gy), likely injury from prompt radiation alone (yellow, > 0.75 Gy) and low probability of injurious health effects from radiation alone (green, < 0.75 Gy).

Section 6.

Discussion

6.1 Analysis of Dose Reduction

The results presented in this report indicate that the radiation transport in the National Capital Region urban setting is more attenuated than previous estimates (Dombroski 2007). The previous estimates determined that the urban environment reduced the radiation to 30% of the open-field radiation. However, the HSRD model revealed that dose reduction is clearly a function of the intervening buildings, as areas of elevated building heights show higher radiation attenuation than areas of lower average building elevation. The model also shows relatively open areas, such as the area in the southern part of the HSRD model, still demonstrating significant attenuation because buildings not in the direct line-of-sight can absorb some of the transporting particles that might have scattered into the open region. There are areas where the simulated urban dose is higher than the open-field dose, but only in areas adjacent to the detonation where scattering from buildings and production of secondary gamma rays from neutron capture is significant.

The impact of the urban landscape reduces the range of an expected lethal exposure outside of buildings to the prompt radiation from approximately 1090 m to 765 m in the west Quadrant and from approximately 1090 m to 910 m in the South Quadrant. In a high-density population center such as Washington, DC, this difference can reduce the radiation and combined injury casualties by almost half, perhaps up to thousands of people. The dose reduction estimates should not be used without an acknowledgement of the variability in the data at any given distance as clearly shown in Figure 5-9 and Figure 5-10. While the mean results can be useful for general planning purposes, emergency-response planners should expect that individuals in the more direct line-of-sight, low-attenuation locations could receive significantly higher doses than the average indicates.

6.1 Recognized HSRD Model Limitations

While the scale and detail of this model representing an urban terrain may be the most complete representation ever developed for use with MCNP at the date of completion, the model still has several limitations which should be recognized when evaluating the results presented in this report. The building materials are still a simple approximation and are not customized for any particular building, even though the buildings do adhere to generic Hazus building types. Also, interior details are not accurately specified, especially when considering the turnover of materials as buildings are renovated. Foliage, vehicles, wall structures and subterranean systems such as culverts, sewers, mass transit, and maintenance tunnels are also not included. The building resolution of 5 m x 5 m x 5 m can overestimate or underestimate the size of the buildings since partially filled lattice elements can be modeled as completely filled with building materials or completely filled with air when only part of the lattice volume is inside the building volume.

6.2 Absorbed Dose versus Equivalent Dose

MCNP can conveniently tally energy-dependent equivalent dose (Sv); however for the model presented here, an absorbed dose (Gy) was deemed the most appropriate value to calculate. The use of absorbed dose allowed for direct comparison of neutron and photon doses, and allowed the doses to be summed to calculate total dose. Further, the primary concern of this work was to best understand the impacts of an urban nuclear-weapon detonation as associated with the possibility of acute, deterministic radiation effects. Equivalent-dose calculations for acute effects are complicated, and the simplified conversion factors that are typically used are more appropriate for estimating longer term, stochastic effects.

It should be noted, though, that the resulting absorbed dose is absorbed dose in tissue, as the conversion factors were originally calculated based on tissue dose. One of the reasons for using tissue dose was it makes the values easier to compare to RERF epidemiological studies.

Section 7.

Conclusions

The results presented in this report suggest the following conclusions based upon the HSRD Monte-Carlo modeling of the prompt radiation emitted by the detonation of a 10-kT fission-type nuclear weapon located at ground level in Washington, DC:

Dose Contribution – For the modeled source spectra at near distances, neutrons are the main contributor to dose as demonstrated in Figure 5-13. However, at increasing distances in both the urban and open-field scenarios, neutron and photon doses begin to converge until the photon dose becomes the greater contributor to the total dose (in this model, the average dose for neutrons and photons is equal at the 500-m radius). In the Hiroshima event, little evidence of injuries from deterministic effects of high-neutron doses has been discovered. However, these simulations show similar levels of prompt radiation dose from photons and neutrons in the survivable injury zone (roughly between 4.1 Gy and 0.75 Gy), without incorporating relative biological effectiveness or internal-organ transmission factors. The effects of large neutron radiation doses may play an important role in consequence-assessment calculations applicable to similar nuclear-detonation scenarios.

Sky-Shine Dose – "Sky-shine", i.e. atmospheric back-scattering of radiation, appears to be dependent on building height. This conclusion can be made by the qualitative observation of Figure 5-5, which serves to depict the total urban-to-open field dose ratio plot. The ratio value is higher on the south quadrant of the plot, corresponding to open spaces, than on the east quadrant, where taller buildings are present. These taller structures effectively shield downward-scattered radiation from the atmosphere. For the regions of the model of the National Capital Region where there was significant building density, the dose was calculated to be reduced, on average, to approximately 17% to 21% of the open-field calculation.

Section 8.

Acknowledgements

We would like to express utmost gratitude to Tim Goorley of Los Alamos National Laboratories. His assistance in running MCNP5 on high-performance computers, sharing input decks of similar problems and reviewing this final document proved to be invaluable.

Section 9.

References

Anno, G. H., R. W. Young, R. M. Bloom, and J. R. Mercier. 2003. "Dose Response Relationships for Acute Ionizing-Radiation Lethality." *Health Physics* 565-575.

DHS. 2003. *National Prepardness Guidelines.* Washington, DC.

Dombroski, Matt, et al. 2007. *Radiological and Nuclear Response and Recover Workshop: Nuclear Weapon Effects in the Urban Environment.* Livermore, CA: Lawrence Livermore National Laboratories.

Federal Emergency Management Agency. 2003. *Multi-hazard loss estimation methodolgy, flood model, HAZUS, technical manual.* technical manual, Washington, DC: Department of Homeland Security, Emergency Preparedness and Response Directorate.

Glasstone, S. and Dolan, P. J. 1977. *The Effects of Nuclear Weapons.* United States Department of Defense and United State Department of Energy.

Goetz, J.L., Klemm, J., Kaul, D. and McGahan, J. T. 1979. *Analysis of Radiation Exposure for Task Force Warrior - Shot Smoky - Exercise Desert Rock VII-VIII Operation Plumbbob.* Washington, D.C.: Defense Nuclear Agency.

HPC Modernization Program. 2013. "HPCMPO Overview 2013 v2." *HPCMP community resources.* June 1. Accessed July 1, 2013. http://www.hpcmo.hpc.mil/cms2/index.php/communityresources.

ICRP (International Commission on Radiological Protection). 1989. *RBE for Deterministic Effects.* Vol. 58. Oxford: Pergamon Press.

ICRP. 1973. *Data for Protection Against Ionizing from External Sources - Supplement to ICRP 15 (ICRP 21).* Oxford, UK: Pergamon Press.

Johnson, J. 2010. *Determination of Atmospheric Conditions over New York City.* Private Communication.

National Aeronautics and Space Administration. 1976. "U. S. Standard Atmosphere, 1976." Washington, DC.

Radiation Effects Research Foundation. 2005. *Reassessment of the Atomic Bomb Radiation Dosimetry for Hiroshima and Nagasaki.* Hiroshima: The Radiation Effects Research Foundation.

White, S. W., Whalen, P. P., and Heath, A. R. 2001. *Source Calculations for the US-Japan Dosimetry Working Group; LA-UR-01-6594.* Los Alamos, NM: Los Alamos National Laboratory.

X-5 Monte Carlo Team,. 2008. *MCNP - A General Monte Carlo N-Particle Transport code, Version 5 (LA-UR-03-1987).* Los Alamos, NM: Los Alamos National Laboratory.

APPENDICES

Appendix A. Atmospheric Composition and Density

The elemental weight fractions of air in and around structures was defined by NIST (National Institute of Standards and Technology), as was the density of 1.20479 mg cm^{-3} for dry air at sea level. These established measurements were adjusted for water-vapor content and density based on elevation as per formulas from "Determination of Atmospheric Conditions over New York City".

Table A-1. Elemental weight fraction of air.

Element	Air @ 0-250 m (1.205 mg cm^{-3})	Air @ 250-500 m (1.205 mg cm^{-3})	Air @ 500-750 m (1.167 mg cm^{-3})	Air @ 750-1000 m (1.117 mg cm^{-3})
H	0.001459	0.001490	0.001524	0.001560
O	0.240904	0.24108	0.241215	0.241505
C	0.000125	0.000124	0.000127	0.000124
N	0.744888	0.744683	0.744224	0.744199
Ar	0.012625	0.012624	0.012911	0.012613

Element	Air @ 1000-1500 m (1.092 mg cm^{-3})	Air @ 1500-2000 m (1.055 mg cm^{-3})	Air @ 2000-2500 m (0.958 mg cm^{-3})
H	0.001614	0.001665	0.001439
O	0.24183	0.242122	0.240772
C	0.000123	0.000123	0.000125
N	0.743823	0.743489	0.745035
Ar	0.01261	0.01260	0.01263

Element	Air @ 2500-3000 m (0.911 mg cm^{-3})	Air @ 3000 - 3500 m (0.866 mg cm^{-3})
H	0.001237	0.001058
O	0.239596	0.23852
C	0.000125	0.000124
N	0.74639	0.747624
Ar	0.012652	0.012673

Appendix B.

MCNP Physics Options

Certain physics options available in MCNP were adjusted to optimize run time and to correctly model nuclear interactions. A 1.0-keV threshold was employed, which artificially removed all photons below this energy from the model. The minimum neutron energy cut-off was determined by the implicit-capture model in MCNP. Analog capture was turned off for both photons and neutrons. The cross-section tables used for each element are listed in Table B-1.

Table B-1. Cross-section information for each element in simulation.

Element Name – Mass Number	MCNP Reference	Cross-section Filename
Hydrogen - 1	1001.70c	ENDF/B-VII njoy99.248
Carbon - Natural Isotope Mix	6000.70c	ENDF/B-VII njoy99.248
Carbon - 12	6012.50c	RMCCS njoy
Nitrogen - 14	7014.70c	ENDF/B-VII njoy99.248
Oxygen - 16	8016.70c	ENDF/B-VII njoy99.248
Sodium - 11	11023.70c	ENDF/B-VII njoy99.248
Aluminum - 13	13027.70c	ENDF/B-VII njoy99.248
Silicon - Natural Isotope Mix	14000.60c	ENDF/B-VI
Sulfur – Natural Isotope Mix	16000.62c	ENDF/B-VI.8 njoy99.50
Argon – Natural Isotope Mix	18000.35c	ENDL85
Potassium – Natural Isotope Mix	19000.62c	ENDF/B-VI.8 njoy99.50
Calcium – Natural Isotope Mix	20000.62c	ENDF/B-VI.8 njoy99.50
Iron – Natural Isotope Mix	26000.55c	RMCCS njoy

Appendix C.

Hazus Building Types

A list of the Hazus building types used by the HSRD Shape2MCNP and MCNP input decks is given in Table C-1. The table lists the Hazus label, an HSRD Number which is given for reference, a description and a concise list of important dimensions. Materials used in this model include concrete, gypsum, glass, carbon steel, brick and wood.

Table C-1. List of different Hazus buildings types listed in model.

Hazus Label	HSRD No.*	Description	Physical Dimensions
W1	4	Wood, Light Frame	Glass=0.5 cm
W2	5	Wood, Commercial and Industrial	Glass=0.5 cm
S1L,S1M,S1H	6	Steel Moment Frame	Concrete floors=8 in, Steel Columns=10 in, Glass = 1 cm
S2L,S2M,S2H	7	Steel Braced Frame	Concrete floors=8 in, Steel Columns=10 in, Glass = 1 cm
S3	8	Steel Light Frame	Concrete floors=8 in, Steel Columns=10 in, Corrugated metal walls=0.2 cm
S4L,S4M,S4H	9	Steel Frame with Cast-in-Place Concrete Shear Walls	Concrete floors=8 in, Steel Columns=10 in, Glass = 1 cm
S5L,S5M,S5H	10	Steel Frame with Unreinforced Masonry Infill Walls	Concrete floors=8 in, Steel Columns=10 in, Glass = 1 cm, brick walls=9 cm
C1L,C1M,C1H	11	Concrete Moment Frame	Concrete floors=8 in, Steel Columns=10 in, Glass = 1 cm
C2L,C2M,C2H	12	Concrete Shear Walls	Concrete floors=8 in, Steel Columns=10 in, Glass = 1 cm
C3L,C3M,C3H	13	Concrete Frame with Unreinforced Masonry Infill Walls	Concrete floors=8 in, Exterior Bricks Walls=9 cm, Glass = 0.5 cm

PC1	14	Precast Concrete Tilt-Up Walls	Wood Floors=5.75 in, Steel Columns=10 in, Glass=1 cm
PC2L,PC2M,PC2H	15	Precast Concrete Frames with Concrete Shear Walls	Concrete Floors=8 in, Glass=1 cm
RM1L, RM1M	16	Reinforced Masonry Bearing Walls with Wood or Metal Deck Diaphragms	Wood Floors=5.75 in, Steel Columns=10 in, Glass=1 cm
RM2L,RM1M,RM2H	17	Reinforced Masonry Bearing Walls with Precast Concrete Diaphragms	Concrete Floors=8 in, Glass=1 cm
URML,URMM	18	Unreinforced Masonry Bearing Walls	Wood=5.75 in, Wood Columns=12 in, Brick Exterior Walls=9 cm, Glass=0.5 cm
MH		Mobile Homes	Same as Wood, Light Frame, Glass=0.5 cm

* HSRD No. is listed for reference.

Abbreviations, Acronyms and Symbols

ARA	Applied Research Associates, Inc.
ArcGIS	Commercially available Geographic Information System from Esri
DC	District of Columbia
DHS	Department of Homeland Security (United States)
DoD	Department of Defense (United States)
DOE	Department of Energy (United States)
DS02	Dosimetry System 2002
DTRA	Defense Threat Reduction Agency (United States)
ESRI	Environmental Science Research Institute
FEMA	Federal Emergency Management Agency (United States)
Gy	Gray radiation dose unit
HHS	Health and Human Services
HSRD	Human Survivability Research and Development Integrated Program Team
ICRP	International Commission on Radiological Protection
IPT	Integrated Program Team
kg	kilogram
LD50/60	Lethal Dose for 50% of population after 60 days
LIDAR	Light detection and ranging, a remote sensing technology
m	meter
MCNP	Monte-Carlo N-Particle radiation transport software
NCR	National Capital Region
NGA	National Geospatial Intelligence Agency
RERF	Radiation Effects Research Foundation
Sv	Sievert radiation dose unit
U.S.	United States